

4th International Conference on Advances in Energy Research 2013, ICAER 2013

Free Rotating Vaneless Diffuser of Diffuser Diameter Ratio 1.30 with Different Speed Ratios and its Effect on Centrifugal Compressor Performance Improvement

Seralathan S^{a,*}, Roy Chowdhury D G^a

^aDepartment of Mechanical Engineering, Hindustan Institute of Technology and Science, Padur 603 103, Tamilnadu, India

Abstract

Free rotating vaneless diffuser is one of the novel methods in the design of radial diffuser for reducing the energy losses associated with diffusion. In the present study, the impeller with a stationary vaneless diffuser of diffuser diameter ratio 1.40 and impeller with a free rotating vaneless diffuser of diffuser diameter ratio 1.30 along with stationary vaneless diffuser at downstream for the remaining radius ratio, running at speed ratios 0.25 and 0.75 times the impeller rotational speed are analyzed. A higher static pressure rise with reduced losses is achieved by free rotating vaneless diffuser configuration, Free RVD30 SR0.75. The static pressure recovery coefficient increased by 23 to 80%, by rotating the diffuser independently over the entire flow range. Also, losses are lesser due to reduced shear between the through flow and independently rotating walls of the diffuser. The efficiency of both Free RVD30 SR0.25 and Free RVD30 SR0.75 are marginally lesser by 3.5 to 5.3% with SVD. This clearly reveals that the diffusion rate is higher in the free rotating vaneless diffuser configuration.

© 2014 S. Seralathan. Published by Elsevier Ltd. This is an open access article under the CC BY-NC-ND license (<http://creativecommons.org/licenses/by-nc-nd/3.0/>).

Selection and peer-review under responsibility of Organizing Committee of ICAER 2013

Keywords: Centrifugal compressor; impeller; free rotating vaneless diffuser; stationary vaneless diffuser

1. Introduction

Novel methods in the design of radial diffuser in reducing the energy losses associated with diffusion necessitate newer diffuser design concepts. Innovative improvements in diffuser design concepts like pipe diffuser, tandem

* Corresponding author. Tel.: +91-944-496-7008

E-mail address: sseralathan@hindustanuniv.ac.in, siva.seralathan@gmail.com

diffuser, etc., have been tried by researchers and one among them is free rotating vaneless diffuser. The stationary vaneless diffuser is replaced with a free rotating vaneless diffuser. In a free rotating vaneless diffuser, the diffuser rotates independently at a speed, fraction to the rotating impeller speed. This is done with a suitable arrangement for rotating the diffuser independently. The shear forces between the through flow and free rotating vaneless diffuser wall is greatly reduced. Also, the boundary layer growth formation with the free rotating vaneless diffuser is much smaller than the corresponding stationary vaneless diffuser.

The free rotating vaneless diffuser developed by Rodgers [1] as well as Rodgers and Mnew [2] in which the walls of the vaneless region are rotated independently of the impeller. A significant improvement in diffuser performance was observed under free rotating conditions with an overall static pressure recovery increase by 20 percent. The overall compressor efficiency increased between four and five percent. Also, frictional losses in the vaneless diffusers of centrifugal compressors reduced by around 70 percent. The effect of rotational speed of a vaneless diffuser on the performance of a centrifugal compressor was discussed by Fradin [3]. The total pressure loss in the stationary vaneless diffuser of a centrifugal compressor is mainly due to fluid friction with the walls. The losses are reduced considerably by rotating the walls of the diffuser at an angular velocity less than that of the impeller. Even though this concept is investigated before [1, 2], further studies by varying the speed ratios i.e., speed of the free rotating vaneless diffuser with respect to impeller rotational speed and its effect on the centrifugal compressor performance is unavailable in the open literature. Also, detailed numerical analysis based on this concept is not available in the open domain. This paper is a part of the series of investigations conducted to study in detail about the fluid mechanics involved with free rotating vaneless diffuser, which helps in documenting and understanding this concept better.

A centrifugal impeller with a diffuser diameter ratio of 1.40 is chosen for the present study. The objective of this present investigations is to study numerically, the impact of free rotating vaneless on the flow diffusion in detail along with the performance characteristics of a centrifugal compressor. The impeller with a stationary vaneless diffuser of diffuser diameter ratio 1.40 (SVD) and impellers with a free rotating vaneless diffuser of diffuser diameter ratio 1.30 along with stationary vaneless diffuser at downstream for the remaining radius ratio running at a speed ratio 0.25 times (Free RVD30SR0.25) as well as speed ratio 0.75 times (Free RVD30 SR0.75) the impeller rotational speed are analyzed with all the other dimensions of the geometrical details remaining the same. The comparative studies are done with the SVD.

Abbreviations

SVD	Impeller with a stationary vaneless diffuser of diffuser diameter ratio 1.40
Free RVD30 SR0.25	Impeller with free rotating vaneless diffuser of diffuser diameter ratio 1.30 with speed ratio 0.25 along with stationary vaneless diffuser at downstream for the remaining radius ratio
Free RVD30 SR0.75	Impeller with free rotating vaneless diffuser of diffuser diameter ratio 1.30 with speed ratio 0.75 along with stationary vaneless diffuser at downstream for the remaining radius ratio
SR 0.25	Speed ratio 0.25 corresponds to the rotational speed of the free rotating vaneless diffuser which is 0.25 times impeller rotational speed
SR 0.75	Speed ratio 0.75 corresponds to the rotational speed of the free rotating vaneless diffuser which is 0.75 times impeller rotational speed

2. Computational Methodology

The dimensional details of the impeller of a low-specific speed centrifugal compressor [4] with different diffuser configurations modeled for the computational study is shown in Table 1. Using ANSYS ICMCFD 13.0, the geometric modeling and grid generation of the computational domain are created. Unstructured grid with tetrahedral elements is generated for the whole computational domain. Flat prism shaped cells in the near wall zones are

introduced to obtain a finer resolution in the boundary layer. Using commercial CFD code, namely ANSYS CFX 13.0, the numerical investigations are carried out. The whole computational domain is defined as rotating frame of reference. Total pressure in stationary frame is given as boundary condition at the inlet. At outlet, mass flow rate is mentioned by considering the number of impeller blades in the computational domain. The boundary conditions [5, 6, 7] specified for the computational domain is shown in the Fig. 1(a) and Fig. 1(b). The blade, hub and shroud are given wall boundary conditions. Side walls of the computational domain are specified as rotational periodic boundary conditions. Suitable interfaces are created between the rotating domains with different rotational speeds as well as between rotating domain and the stationary domain. The stationary domain is specified as counter rotating type. The free rotating vaneless diffuser domain is specified with speed which is a fraction of the impeller speed. No-slip conditions are enforced on the blade, hub and shroud. By assuming as a smooth wall, the wall roughness is neglected. The turbulence is modeled using $k-\omega$ model. The convergence criteria of RMS residuals for all the governing equations are resolved to 1×10^{-4} . The results from the numerical study are validated with the available experimental results [4].

Table 1. Dimensional details of centrifugal impeller [4], free rotating vaneless diffuser and stationary vaneless diffuser

Centrifugal Impeller			Stationary Vaneless Diffuser		
Diameter at exit of the impeller	D_2	570 mm	Diffuser outlet diameter	D_4	798 mm
Diameter at inlet of the impeller	D_1	215.2 mm	Diffuser inlet diameter	D_3	570 mm
Outer diameter to inner diameter ratio	D_2/D_1	2.649	Diffuser diameter ratio	D_4/D_3	1.40
Number of blades	Z	18	Free Rotating Vaneless Diffuser		
Width of the blade at exit	b_2	27.6 mm	Free RVD inlet	D_{3*}	570 mm
Width of blade at inlet	b_1	58.5 mm	Free RVD outlet	D_{3**}	741 mm
Thickness of the blade	T	6 mm	SVD inlet	D_3	741 mm
Blade angle at the inlet	β_1	44.6°	SVD outlet	D_4	798 mm
Blade angle at the exit	β_2	90°	SR0.25 – Speed Ratio 0.25 (375 rpm)		
Rotational speed of the impeller	N	1500 rpm	SR0.75 – Speed Ratio 0.75 (1125 rpm)		

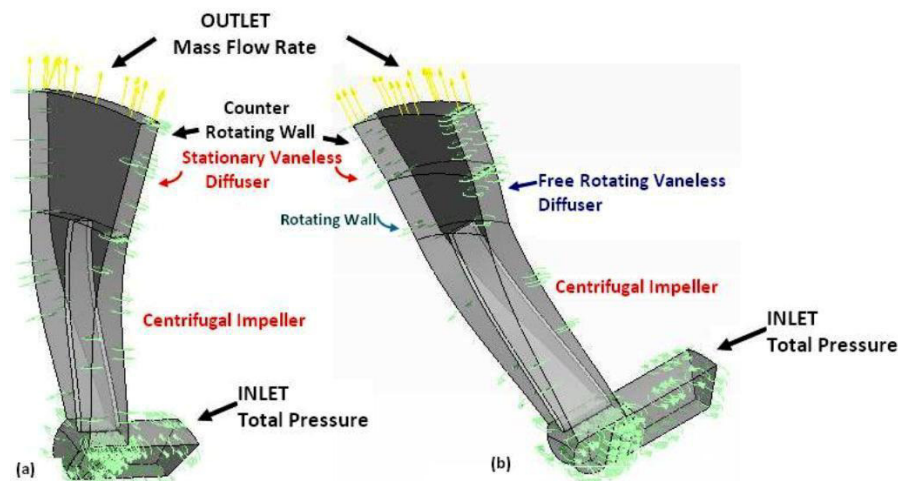


Fig.1. (a) Boundary conditions for the centrifugal impeller with stationary vaneless diffuser; (b) Boundary conditions for the impeller with free rotating vaneless diffuser

3. Results and Discussions

The flow through the diffuser configurations (SVD, Free RVD30 SR0.25 and Free RVD30 SR0.75) are analyzed for four different flow coefficients at design and above design conditions. The results for efficiency, energy coefficient, static pressure recovery coefficient, stagnation pressure loss coefficient and static pressure as well as stagnation pressure are presented here and the comparison are done with an impeller with a stationary vaneless diffuser (SVD) for the present study.

The performance characteristics of the centrifugal compressor with different diffuser configurations at a design speed of 1500 rpm for efficiency (η) and energy coefficient (ψ) against flow coefficient, Φ where $\Phi = C_m/U_2$, where C_m is meridional velocity and U_2 is peripheral velocity at outlet, are shown in Fig. 2(a) and Fig. 2(b). The efficiency decreases with increase in flow coefficients for all the configurations. The efficiencies of SVD are higher than Free RVD30 SR0.25 and Free RVD30 SR0.75 at design flow coefficient as well as in off-design conditions. Energy coefficient, ψ , defined as $2W/U_2^2$, where W is specific work, is a measure of the pressure rise in the centrifugal compressor, is highest for Free RVD30 SR0.75 followed by Free RVD30 SR0.25. In all the cases, the energy coefficient of free rotating vaneless diffuser is higher than SVD for entire range of flow coefficients.

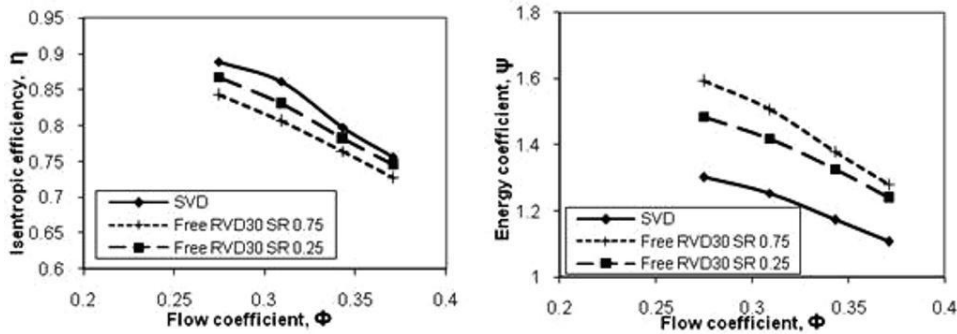


Fig. 2. (a) Variation of isentropic efficiency for SVD, Free RVD30 SR0.25 and Free RVD30 SR0.75 configurations with flow coefficient; (b) Variation of energy coefficient for SVD, Free RVD30 SR0.25 and Free RVD30 SR0.75 configurations with flow coefficient

The static pressure recovery coefficient, ψ_p , is defined as $2(P - P_2)/\rho U_2^2$, where P_2 and P are mass averaged static pressure at impeller exit and diffuser exit respectively. The variation of static pressure recovery coefficient against flow coefficient is shown in Fig. 3(a).

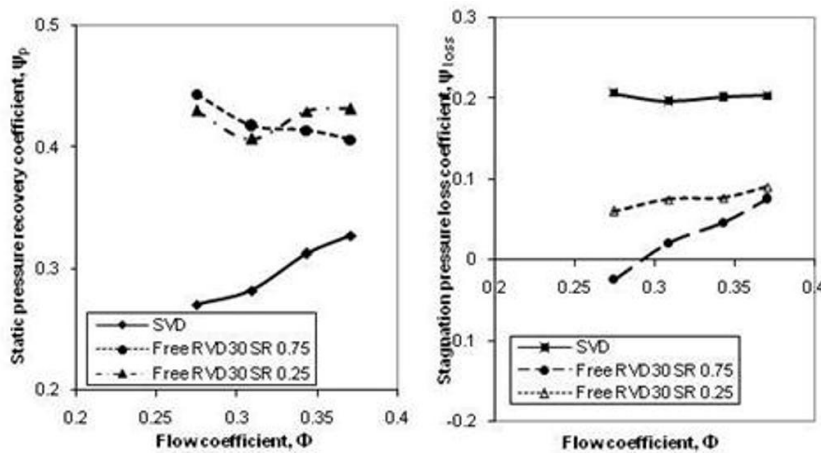


Fig. 3. (a) Variation of static pressure recovery coefficient for SVD, Free RVD30 SR0.25 and Free RVD30 SR0.75 configurations with flow coefficient; (b) Variation of stagnation pressure loss coefficient for SVD, Free RVD30 SR0.25 and Free RVD30 SR0.75 configurations with flow coefficient

The static pressure recovery for free rotating vaneless diffuser configurations is higher than SVD by around 23 to 80% over the entire range of flow coefficient. The static pressure rise is highest at design condition for Free RVD30 SR0.75 and at off-design conditions for Free RVD30 SR0.25, which is also higher than SVD. This reveals that diffusion rate is higher in the free rotating vaneless diffuser configurations than SVD. The stagnation pressure loss coefficient, ψ_{loss} is defined as $2(P_{02} - P_0)/\rho U_2^2$, where P_{02} and P_0 are mass averaged stagnation pressure at impeller exit and diffuser exit respectively. The variation of stagnation pressure loss coefficient against flow coefficient is

shown in Fig. 3(b). The stagnation pressure loss coefficient for SVD remains almost same for wide range of flow coefficient whereas for free rotating vaneless diffuser configurations, the loss at design flow rate is lowest and it gradually increases for above design conditions. The stagnation pressure loss coefficient for SVD is higher than the free rotating vaneless diffuser configurations for the entire range of flow coefficients, indicating the amount of losses occurring in the flow passage due to friction. The additional energy imparted to the fluid by the independently rotating walls of the free rotating vaneless diffuser has resulted in additional energy gain as seen in the Fig. 3(b). The losses in the free rotating vaneless diffuser are lesser due to reduced shear between the through flow and independently rotating walls of the diffuser. The boundary layer growth in the independently rotating walls of the diffuser is smaller in comparison with SVD. This effectively contributes in improving the centrifugal compressor performance for the configurations with free rotating vaneless diffuser configurations.

3.1. Static Pressure Distribution

The static pressure in general increases with increase in radius ratio due to flow diffusion. The static pressure distribution across the width from impeller exit to the diffuser exit is presented in a non-dimensional form as static pressure coefficient, $C_p = P_s / (\rho/2)U_2^2$, where P_s is the static pressure, U_2 is the impeller exit peripheral velocity and ρ is the density of air, in Fig. 4 (a), (b) and (c) for various flow coefficients.

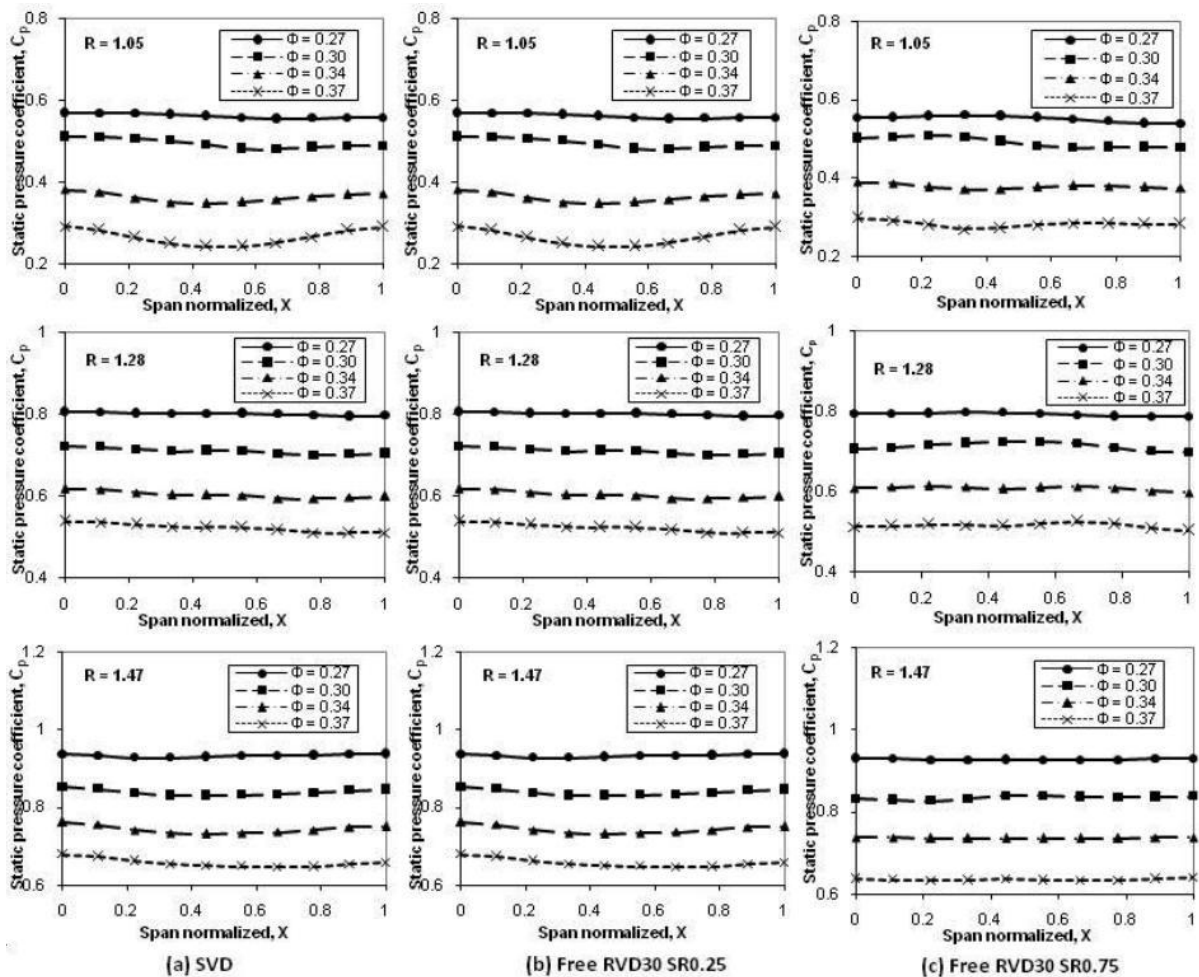


Fig. 4. (a), (b) and (c) Variation of static pressure coefficient with flow coefficient for SVD, Free RVD30 SR0.25 and Free RVD30 SR0.75 measured across the width of the impeller and diffuser at various radius ratios $R = 1.05$, $R = 1.28$ and $R = 1.47$

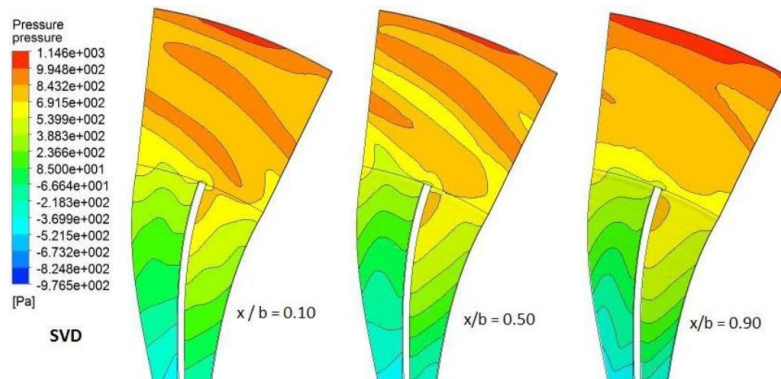


Fig. 5. Contours of static pressure distribution for SVD on the axial plane at $x/b = 0.10, 0.50$ and 0.90 at design flow coefficient, $\Phi = 0.27$

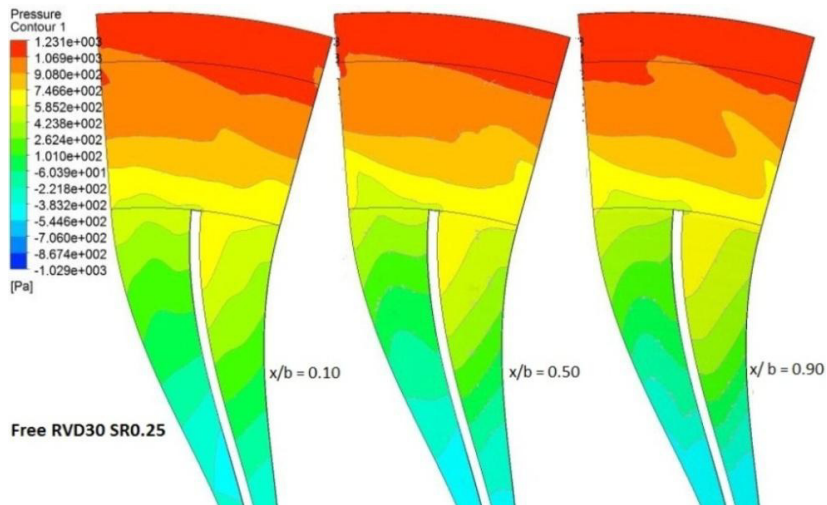


Fig. 6. Contours of static pressure distribution for Free RVD30 SR0.25 on the axial plane at $x/b = 0.10, 0.50$ and 0.90 at $\Phi = 0.27$

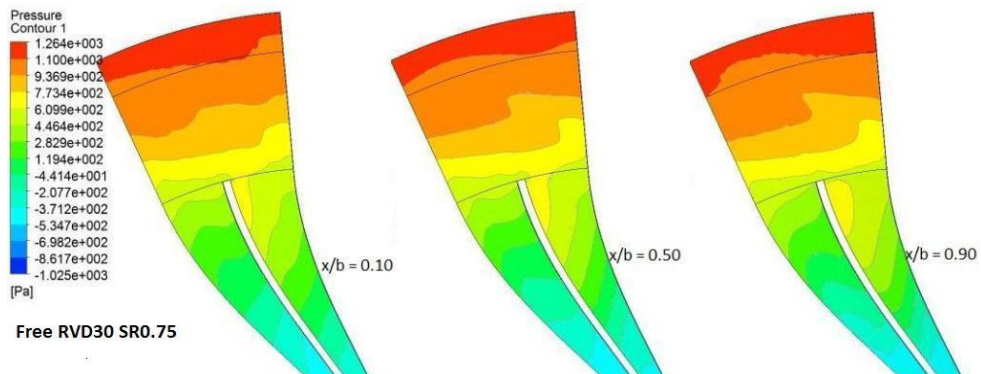


Fig. 7. Contours of static pressure distribution for Free RVD30 SR0.75 on the axial plane at $x/b = 0.10, 0.50$ and 0.90 at $\Phi = 0.27$

As the flow coefficient is reduced, the magnitude of the static pressure at any section increases, similarly to the stagnation pressure distribution. Both Free RVD30 SR0.75 and Free RVD30 SR0.25 offers almost same static pressure rise at $\Phi = 0.27$ and $\Phi = 0.30$, which are however higher than the static pressure rise in SVD. This is also

reflected with higher static pressure recovery coefficient at the exit of the diffuser, which reveals that the rate of diffusion is much higher in free rotating vaneless diffuser configurations compared to SVD. Further, the free rotating vaneless diffusers tend to smooth out distorted entry flow profiles, thereby inducing higher performances for the downstream diffusion system.

The contours of static pressure distribution on the axial plane from hub to shroud at near the impeller hub wall ($x/b = 0.10$), mid axial location ($x/b = 0.50$) and near the impeller shroud wall ($x/b = 0.90$) for design flow coefficient, $\Phi = 0.27$, are shown in Figure 5, 6 and 7 for SVD, Free RVD30 SR0.25 and Free RVD30 SR0.75 respectively. From the contours, it is clear that Free RVD30 SR0.25 and Free RVD30 SR0.75 offers almost equivalent static pressure rise at design flow coefficient, which is higher than SVD. Free RVD30 SR0.75 gives a slightly better static pressure distribution than Free RVD30 SR0.25 by around 2.40 to 4.10%.

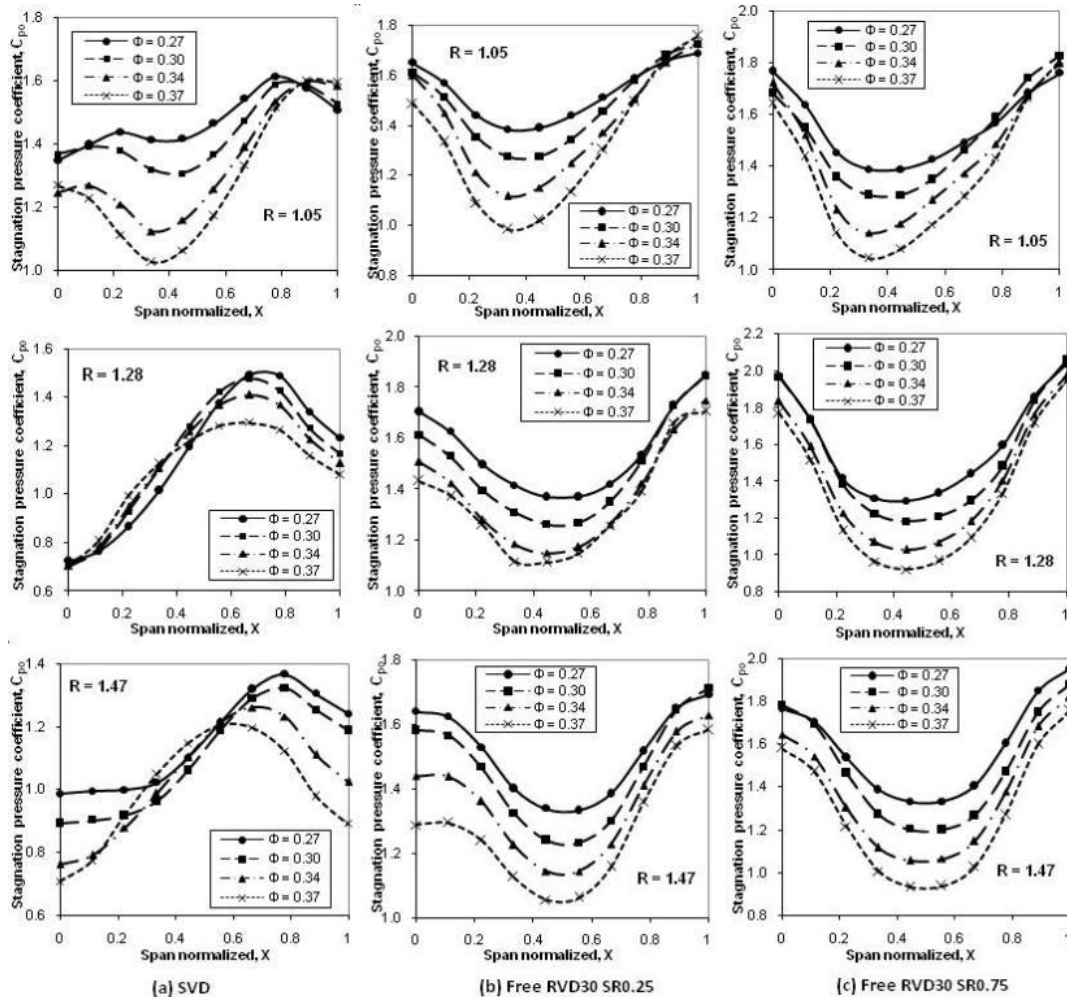


Fig. 8. (a), (b) and (c) Variation of stagnation pressure coefficient with flow coefficient for SVD, Free RVD30 SR0.25 and Free RVD30 SR0.75 measured across the width of the impeller and diffuser at various radius ratios $R = 1.05, R = 1.28$ and $R = 1.47$

3.2. Stagnation Pressure Distribution

The stagnation pressure decreases with increase in flow coefficient for all the configurations. Also, the stagnation pressure decreases as the radius ratio increases for all the flow coefficients. The stagnation pressure distribution

measured across the width from impeller exit to the diffuser exit is presented in a non-dimensional form as stagnation pressure coefficient, $C_{p0} = P_0 / (\rho/2)U_2^2$, where P_0 is the stagnation pressure, in Fig. 8 (a), (b) and (c) with flow coefficients.

The decrease in stagnation pressure indicates the amount of losses that occurs within the flow passage. The stagnation pressure drop is more for SVD, which indicates the higher amount of frictional losses occurring along the walls in the stationary vaneless diffuser passage whereas in Free RVD30 SR0.25 configuration, the shear losses between the wall and through flow in the passage is considerably reduced due to independently rotating vaneless diffuser walls at a speed ratio of 0.25 times impeller speed which is reflected with lesser total pressure drop in Fig. 8 (b). In Free RVD30 SR0.75, the fall in stagnation pressure drop are drastically reduced due to reduced shear losses between the free rotating walls at a speed ratio 0.75 and through flow and also by the additional energy imparted to the fluid by independently rotating walls of the diffuser. Also, at radius ratio $R = 1.47$, the variations of the stagnation pressure distribution for free rotating vaneless diffuser configuration is identical in pattern for wide range of flow coefficients at design and off-design conditions.

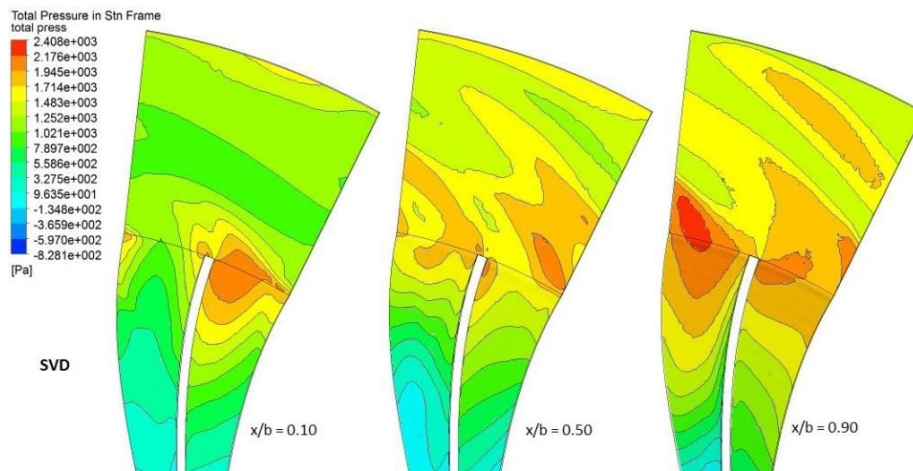


Fig.9. Contours of stagnation pressure distribution for SVD on the axial plane at $x/b = 0.10, 0.50$ and 0.90 at $\Phi = 0.27$

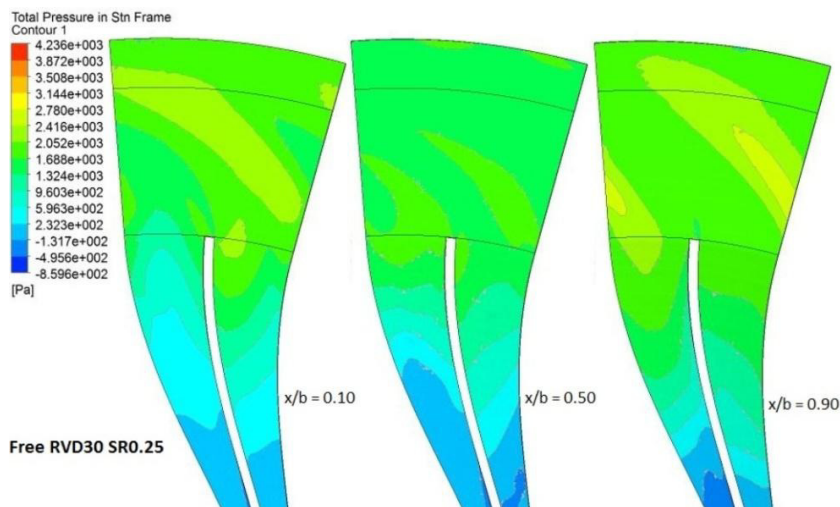


Fig. 10. Contours of stagnation pressure distribution for Free RVD30 SR0.25 on the axial plane at $x/b = 0.10, 0.50$ and 0.90 at $\Phi = 0.27$

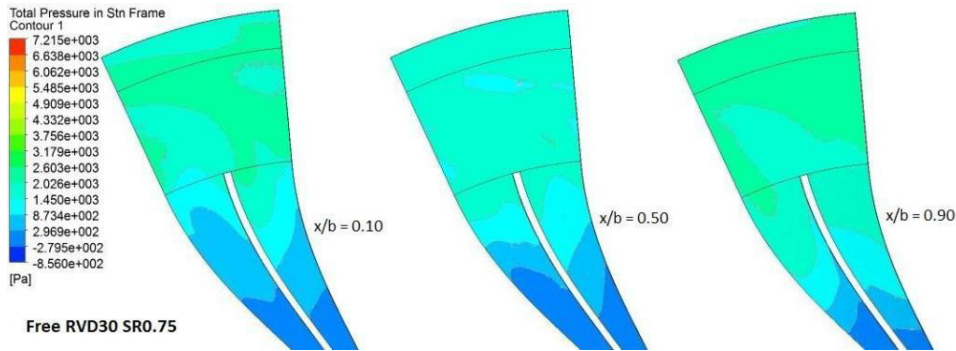


Fig. 11. Contours of stagnation pressure distribution for Free RVD30 SR0.75 on the axial plane at $x/b = 0.10, 0.50$ and 0.90 at $\Phi = 0.27$

The contours of stagnation pressure distribution on the axial plane from hub to shroud at near the hub wall ($x/b = 0.10$), mid axial location ($x/b = 0.50$) and near the shroud wall ($x/b = 0.90$) for design flow coefficient, $\Phi = 0.27$, are shown in Figure 9, 10 and 11 for SVD, Free RVD30 SR0.25 and Free RVD30 SR0.75 respectively. From the above contours, it is evident that the SVD has the drastic drop in stagnation pressure due to higher shear losses between the through flow and the walls of the stationary vaneless diffuser. In free rotating vaneless diffuser concepts, the shear losses are significantly reduced.

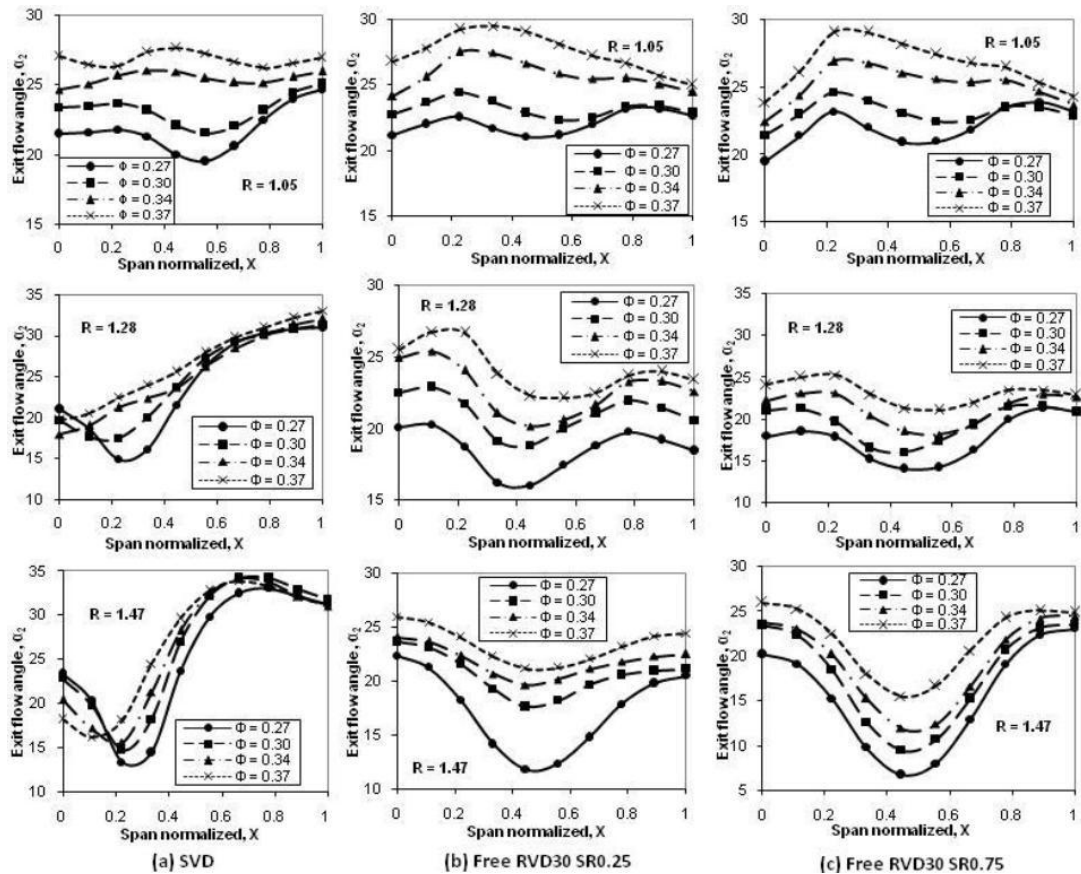


Fig. 12. (a), (b) and (c) Variation of exit flow angle with flow coefficient for SVD, Free RVD30 SR0.25 and Free RVD30 SR0.75 measured across the width of the impeller and diffuser at various radius ratios $R = 1.05, R = 1.28$ and $R = 1.47$

3.3. Exit Flow Angle

The variations of exit flow angle (α_2) across the width from impeller exit to the diffuser exit with various flow coefficients are presented in Fig. 12 (a), (b) and (c) for SVD, Free RVD30 SR0.25 and Free RVD30 SR0.75. The flow angle increases with increase in flow coefficients for all the diffuser configurations. The flow angle increases with radius ratio for the SVD configuration. In free rotating vaneless diffuser configurations, the flow angle of Free RVD30 SR0.75 is slightly lesser than Free RVD30 SR0.25. Also, the pattern of distribution of flow angle in free rotating vaneless diffuser configurations is almost similar for various flow coefficients across the radius ratio. The smaller values of flow angle obviously indicates a smaller meridional velocity component of absolute velocity and for higher values of flow angle, the meridional velocity will accordingly be higher. From the Figure 12 (b) and (c), the free rotating vaneless diffusers tend to smooth out distorted entry flow profiles, thereby inducing higher performances for downstream diffusion system.

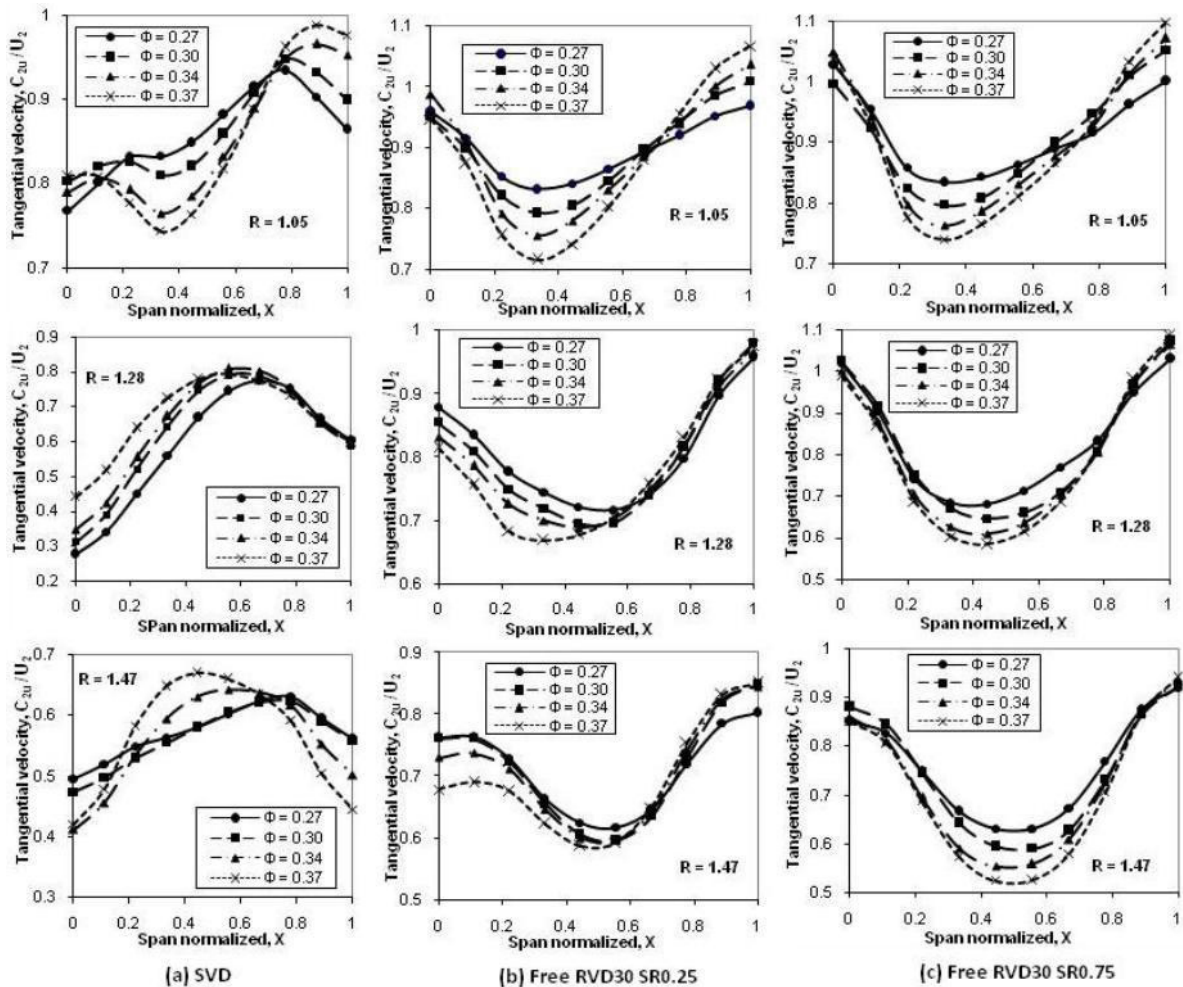


Fig. 13. (a), (b) and (c) Variation of tangential velocity distribution with flow coefficient for SVD, Free RVD30 SR0.25 and Free RVD30 SR0.75 measured across the width of the impeller and diffuser at various radius ratios $R = 1.05$, $R = 1.28$ and $R = 1.47$

3.4. Tangential Velocity Distribution

The tangential velocity distribution across the width from impeller exit to the diffuser exit with various flow coefficients is presented in Fig. 13 (a), (b) and (c) for SVD, Free RVD30 SR0.25 and Free RVD30 SR0.75. The

variation of tangential velocity distribution is almost similar to absolute velocity distribution. The reduction of the tangential velocity component from exit of the impeller to the diffuser exit results in static pressure rise along the diffuser path. Also, there is a reduction in tangential velocity with the increase in radius at all flow coefficients. The magnitude of tangential velocities of Free RVD30 SR0.75 are higher than SVD for all the flow rates and also with the reduction of tangential velocity component from impeller exit to diffuser exit, resulting in higher static pressure rise as seen in Figure 4(c) and Figure 7.

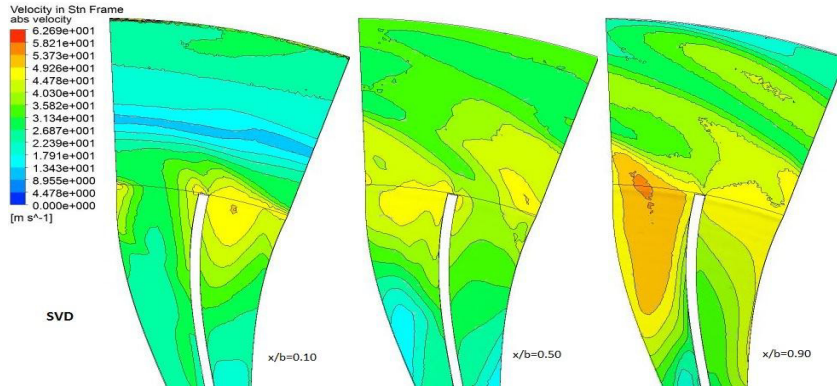


Fig.14. Contours of absolute velocity distribution for SVD on the axial plane at $x/b = 0.10, 0.50$ and 0.90 at $\Phi = 0.27$

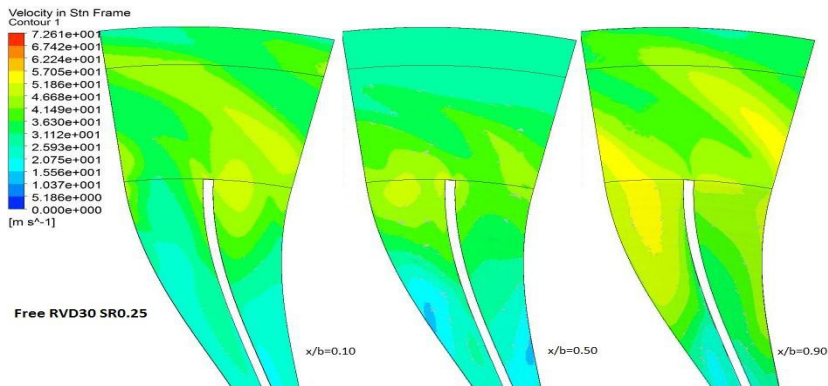


Fig.15. Contours of absolute velocity distribution for Free RVD30 SR0.25 on the axial plane at $x/b = 0.10, 0.50$ and 0.90 at $\Phi = 0.27$

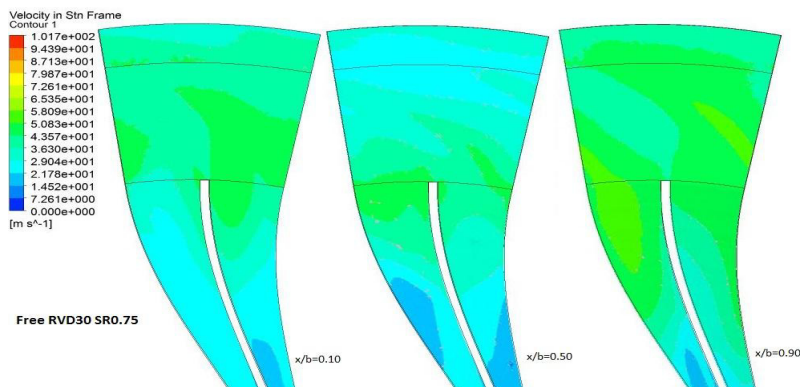


Fig.16. Contours of absolute velocity distribution for Free RVD30 SR0.75 on the axial plane at $x/b = 0.10, 0.50$ and 0.90 at $\Phi = 0.27$

3.5. Absolute Velocity Distribution

The contours of absolute velocity distribution on the axial plane from hub to shroud at near the hub wall ($x/b = 0.10$), mid axial location ($x/b = 0.50$) and near the shroud wall ($x/b = 0.90$) for design flow coefficient, $\Phi = 0.27$, are shown in Figure 14, 15 and 16 for SVD, Free RVD30 SR0.25 and Free RVD30 SR0.75 respectively. The quantity of decrease in absolute velocity depends upon the effectiveness of the diffusion process. As the radius ratio increases, absolute velocity decreases for all the configurations. But, the decrease in absolute velocity is more in the Free RVD30 SR0.75 which is reflected in the order of static pressure rise as observed in Figure 4(c) and Figure 7.

4. Conclusions

The performance characteristics of diffuser configurations involving free rotating vaneless diffuser (Free RVD30 SR0.25 and Free RVD30 SR0.75) are analyzed in terms of efficiency, energy coefficient, stagnation pressure loss coefficient, static pressure recovery coefficient as well as static pressure rise. The following conclusions are obtained based on the results.

- A higher static pressure rise with reduced losses is achieved by Free RVD30 SR0.75 configuration.
- The static pressure recovery coefficient increased by around 23 to 80% over the entire flow range, by independently rotating the vaneless diffuser at a speed ratio of 0.75 times the impeller rotational speed.
- The losses in the free rotating vaneless diffuser (Free RVD30 SR0.75) are lesser due to reduced shear between the through flow and independently rotating walls of the diffuser. At design flow condition, there is a gain in energy to the fluid by the freely rotating vaneless diffuser.
- The efficiency of Free RVD30 SR0.75 configuration is marginally lesser by around 5.3 to 6.3% with SVD at design and off-design flow coefficients.
- The energy coefficient, which is a measure of pressure rise in the compressor, increased by around 17 to 23% for Free RVD30 SR0.75 configuration over the entire flow range.
- The free rotating vaneless diffuser smooth out the distorted entry flow profiles thereby improving the performance of the downstream diffusion system.

This indicates that rate of diffusion is higher in the free rotating vaneless diffuser configuration. By the comparing the performance characteristics of free rotating vaneless diffuser configuration with speed ratio 0.25 (Free RVD30 SR0.25) and speed ratio 0.75 (Free RVD30 SR0.75), the performance improvement for the centrifugal compressor in terms of static pressure rise with reduced losses is enhanced with speed ratios above 0.25 times the impeller rotational speed. Thus, the free rotating vaneless diffuser concept can be put into practice in low-specific speed centrifugal compressors for achieving a higher static pressure rise with reduced losses.

References

- [1] Rodgers C. Analytical experimental and mechanical evaluation of free rotating vaneless diffuser, Final report, ER 2391, AD 744475; 1972.
- [2] Rodgers C, Mnew H. Experiments with a model free rotating vaneless diffuser. ASME Journal of Engineering for Power 1975;231-244.
- [3] Fradin C. The effect of the rotational speed of a vaneless diffuser on the performance of a centrifugal compressor, European space agency, Paris, Report no: ESA-TT-202 ONERA-NT-218; 1975.
- [4] Govardhan M, Moorthy BSN, Gopalakrishnan G, 1978. A preliminary report on the rotating vaneless diffuser for a centrifugal impeller, Proceedings of the first international conference on centrifugal compressor technology, Indian Institute of Technology Madras, Chennai, India.
- [5] Govardhan M, Seralathan S. Effect of forced rotating vaneless diffusers on centrifugal compressor stage performance. Journal of Engineering Science and Technology 2011;6(5):558-574.
- [6] Seralathan S, Roy Chowdhury DG. Modification of centrifugal impeller and effect of impeller extended shrouds on centrifugal compressor performance. Procedia Engineering 2013;64:1119-1128.
- [7] Seralathan S, Roy Chowdhury DG. Computational study on the effect of blade cutback on the performance of the centrifugal compressor. Procedia Technology 2013;10:400-408.